ELECTRON CLOUD AND COLLECTIVE EFFECTS IN THE INTERACTION REGION OF FCC-ee

E. Belli[1,2*], M. Migliorati[1], G. Rumolo[2]
[1] University of Rome 'La Sapienza' and INFN Sez. Roma1, Rome, Italy
[2] CERN, Geneva, Switzerland

Abstract

The FCC-ee is an e^+e^- circular collider designed to accommodate four different experiments in a beam energy range from 91 GeV to 350 GeV and is a part of the Future Circular Collider (FCC) project at CERN. One of the most critical aspects of this new very challenging machine regards the collective effects which can produce instabilities, thus limiting the accelerator operation and reducing its performance. The following studies are focused on the Interaction Region of the machine. This paper will present preliminary simulation results of the power loss due to the wake fields generated by the electromagnetic interaction of the beam with the vacuum chamber. A preliminary estimation of the electron cloud buildup is also reported, whose effects have been recognized as one of the main limitations for the Large Hadron Collider at CERN.

INTRODUCTION

The Future Circular Lepton Collider FCC-ee has been designed as an e^+e^- collider with a centre-of-mass energy from 91 to 350 GeV and 100 km circumference. In this paper we will focus on the Interaction Region (IR) of the machine, whose proposed layouts are shown in Fig. 1. While the symmetric layout [1] has synchrotron radiation (SR) masks to shield the two final focusing quadrupoles and a 12mm pipe radius , the asymmetric layout [2] presents two ingoing pipes with 13mm radius and two outgoing pipes with a larger radius of 20mm. In particular, this latter design will allow high order modes that remain trapped in the IR to escape to the outside through the outgoing pipes, whose cutoff frequancy is the same as the IP. Moreover, in the asymmetric optics the final quadrupole closer to the IP is thinner and stronger. High Order Modes (HOMs) and electron cloud studies presented in this paper will be focused on both the layouts, since there are still many open questions. Regarding all the FCC-ee beam pipes (including those at IR), it was decided to use them at room temperature as in the case of KEKB, SuperKEKB and other lepton colliders. However, even if there will be no cryogenic systems, the beam heat load represents one of the major issues to be analyzed in the machine, in order to avoid extra heating and eventual damage of the background.

By considering a uniformly filled machine, i.e. a train of M bunches covering the full ring circumference ($M = h$ with h the harmonic number) with bunch spacing $\tau_b = \frac{2\pi}{h\omega_0}$ where ω_0 is the revolution frequency, the total power loss of the beam depends only on the real part of the longitudinal component of the coupling impedance [3]:

$$P_{loss} = I^2 \sum_{p=-\infty}^{+\infty} |\Lambda(pM\omega_0)|^2 Re[Z_\parallel(pM\omega_0)] \qquad (1)$$

where Λ is the bunch spectrum, $Re[Z_\parallel]$ is the real part of the longitudinal impedance and $I = \frac{MNe}{T_0}$ is the average beam current with N the bunch population and T_0 the revolution period of the machine.

Possible beam heat load sources in the IR are the resistive wall wake fields, geometric wake fields due to the step transitions of the SR masks, the HOMs that remain trapped in the IR and the electron cloud in the two final focusing quadrupoles.

IMPEDANCE STUDIES

This section will present preliminary results of the power losses due to geometrical and resistive wall impedances and trapped modes carried out by analytical tools and simulation codes.

Heat Load due to Resistive Wall Impedance

The resistive wall impedance is produced by the finite resistivity of the beam pipe. If we consider a circular pipe with radius b the classic analytic formula for the power loss per unit length due to resistive wall is given by:

$$\frac{P_{loss}}{L} = \frac{1}{T_0} \frac{N^2 e^2 c}{4\pi^2 b \sigma_z^{\frac{3}{2}}} \sqrt{\frac{Z_0}{2\sigma_c}} \Gamma\left(\frac{3}{4}\right) n_b \qquad (2)$$

where N is the bunch population, e the elementary charge, σ_z the bunch length, σ_c the conductivity of the material, Z_0 the vacuum impedance and n_b the number of bunches. In the evaluation of the resistive wall impedance, we considered a beam pipe with 12mm radius and three layers: a first layer of aluminum or copper with 2mm thickness, then 2mm of dielectric and finally stainless steel with resitivity $6.89 \cdot 10^{-7} \Omega m$. Simulations were performed by using the Impedancewake2D code [4] and results are shown in Fig. 2, for both the aluminum (with a conductivity $\sigma_{Al} = 3.77 \cdot 10^7 S/m$) and copper (with conductivity $\sigma_{Cu} = 6 \cdot 10^7 S/m$). The results for the power loss are summarized in Table 1 for the two energy cases of 45.6 GeV and 175 GeV at the nominal beam parameters.

* eleonora.belli@cern.ch

ISBN 978-3-95450-187-8

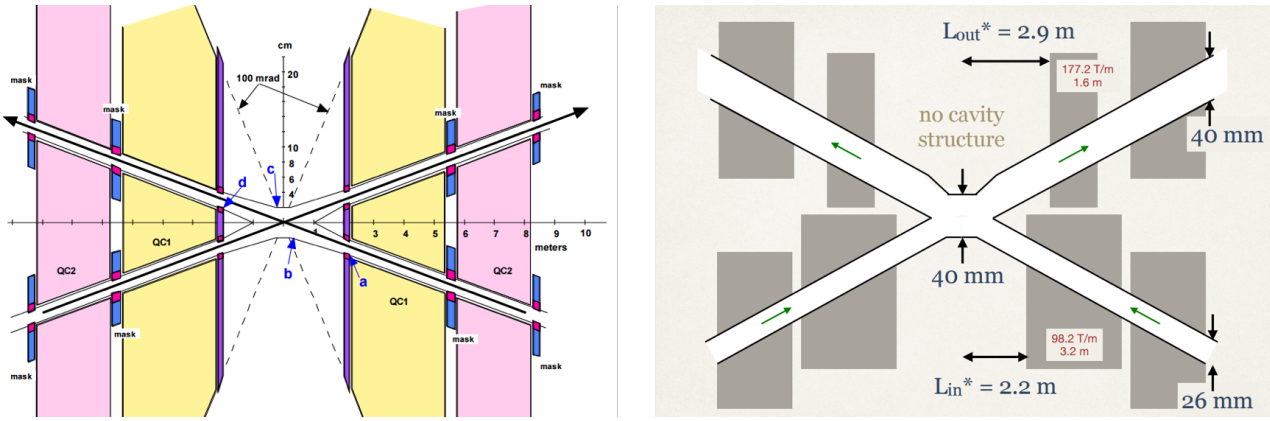

Figure 1: The IR symmetric layout [1] (on the left) and the IR asymmetric layout [2] (on the right).

Table 1: Power Loss Due to Resistive Wall Impedance

Energy [GeV]	**45.6**		**175**
Bunch spacing [ns]	7.5	2.5	4000
Bunch population [10^{11}]	1.0	0.33	1.7
Bunches/beam	30180	91500	81
Bunch length [mm]	6.7	3.8	2.5
P_{loss} [W/m](Al)	74.11	57.25	2.52
P_{loss} [W/m](Cu)	59	45.58	2

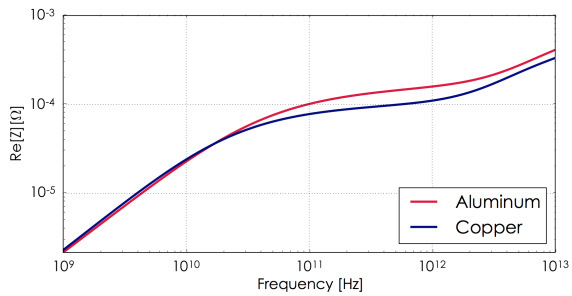

Figure 2: Resistive wall impedance for aluminum (in red) and copper (in blue).

Heat Load due to Geometric Impedance

When there is a geometric variation of the vacuum chamber and the beam passes through a section of a circular pipe from a radius a to a radius b, wake fields are produced at the edges of the discontinuity to satisfy the new boundary conditions. In particular, when the beam goes into a narrower pipe (step-in transition), the real part of the impedance is negative and shows a peak at the cutoff frequency of the larger pipe, while it vanishes above cutoff. On the other hand in the step-out case, i.e. when the beam enters a larger pipe, the real part of the impedance is mostly resistive with a peak at cutoff and then it reaches an asymptotic value. Thus, above cutoff the real part of the impedance is:

$$\begin{aligned} Re[Z^{in}] &\simeq 0 \\ Re[Z^{out}] &\simeq \frac{Z_0}{\pi} ln\left(\frac{b}{a}\right) \end{aligned} \tag{3}$$

Theoretical studies [5] show that at low frequencies the geometric impedance is purely inductive (the real impedances of the step-in and the step-out cancel out) and in the case of step length l greater than the pipe radius b, the impedance is given by the contribution of two independent transition steps:

$$Z(\omega) = 2j\omega \frac{Z_0}{4bc}\left[h^2 + \frac{lh}{\pi}\left(2ln\left(\frac{8\pi l}{h}\right) - 3\right)\right] \tag{4}$$

where h is the difference between the two pipe radii. As shown in the symmetric layout in Fig. 1, masks are placed after each quadrupole to shield the magnet from synchrotron radiations. These masks are 20cm long and produce a variation of 2mm in the pipe radius (from 12mm to 10mm). Geometric impedances and wake potentials have been computed with the ABCI code [6]. In particular Fig. 3 shows the wake potential obtained from ABCI for the lowest energy case: by considering a circular pipe of 12mm radius and the nominal bunch length $\sigma_z = 3.8mm$, we obtain a loss factor $k_l = 6.386 \cdot 10^{-2} V/pC$ which corresponds to a power loss per bunch of $P_{loss} = 5.4mW$. Table 2 shows the total power loss due to geometric impedance for the lowest and highest energy cases at the nominal bunch length.

Table 2: Power Loss due to Geometric Impedance

Energy [GeV]	**45.6**		**175**
Bunch population [10^{11}]	1.0	0.33	1.7
Bunches/beam	30180	91500	81
Bunch spacing [ns]	7.5	2.5	4000
Bunch length [mm]	6.7	3.8	2.5
k [V/pC]	8.077 10^{-3}	6.38 10^{-2}	1.93 10^{-1}
P_{loss} [W]	189.1	493.2	35

ISBN 978-3-95450-187-8

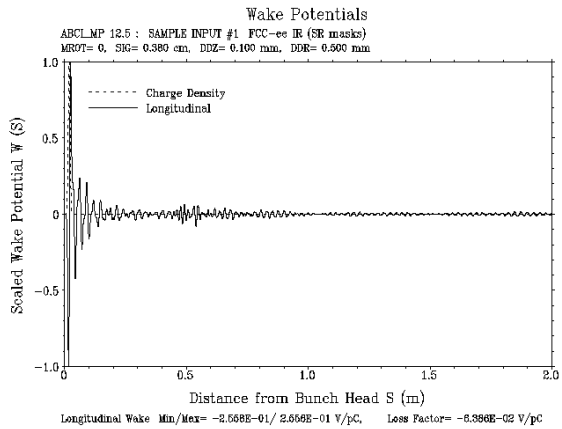

Figure 3: Wake potential of σ_z=3.8mm bunch at 45.6 GeV given by SR masks.

Heat Load due to Trapped Modes

It is well known from the theory [7] that small variations in the beam pipe geometry can generate accidental cavities and produce trapped modes, i.e. resonance peaks with frequencies below the cutoff frequency of beam pipe. These modes cannot propagate into the pipe and remain localized near the discontinuity, representing another possible source of heating that must be analyzed with particular care. As mentioned at the beginning of this paper, the final choice of the FCC-ee Interaction Region layout will be mainly based on HOMs considerations. The asymmetric design proposed in [2] will allow the trapped modes to escape to the outside through the outgoing pipes, thanks to the same radius of the IP. CST eigenmode and impedance simulations in the frequency domain confirmed the presence of a large number of trapped modes in the interaction region. In this section, we will present preliminary simulation results for TM modes trapped in the IR and the resulting power loss. A general method that can be followed to study the HOMs in the IR is the following:

- Build a CST 3D model of the interaction region
- Wakefield simulations (time domain)
- Eigenmode simulations (frequency domain)
- For each excited mode, extract parameters (resonance frequency ω_r, shunt impedance R_s and quality factor Q) and evaluate the real part of the impedance as:

$$Z(\omega) = \frac{R_s}{1 + iQ(\frac{\omega_r}{\omega} - \frac{\omega}{\omega_r})} \quad (5)$$

- Compute the power loss by following the model given by equation 1

Fig. 4 shows the real part of the longitudinal impedance obtained from CST wakefield simulations for the symmetric layout. The peaks of impedance correspond to the modes excited in the pipe below the cutoff frequency of the outgoing

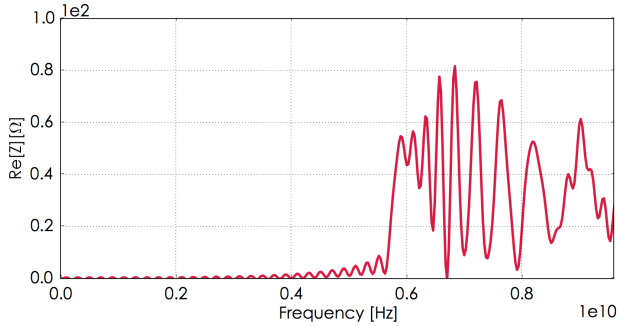

Figure 4: Real part of the longitudinal impedance in the symmetric layout case.

pipes that could remain trapped in the interaction region and represent an issue in terms of extra heating. In the symmetric layout case, the cutoff frequency of the outgoing pipes with 12mm radius is around $f_{cutoff} = 9.57GHz$ for TM_{01} modes. By assuming that all the TM modes below this cutoff are excited and remain trapped in the IR, we obtain a total power loss (given by the contribution of each mode) $\simeq$ 2.74W. In the case of the asymmetric layout, the cutoff frequency of the outgoing pipes with 20mm radius is around $f_{cutoff} = 5.74GHz$ for TM_{01} modes. As expected, eigenmode simulations showed that there are no longitudinal modes below cutoff trapped in the interaction region and this was also confirmed with wakefield simulations.
Trapped modes can also excite longitudinal coupled bunch instabilities. Fig. 5 shows the maximum shunt impedance of a HOM as a function of its resonance frequency giving an instability growth rate which is compensated by the natural radiation damping [8].

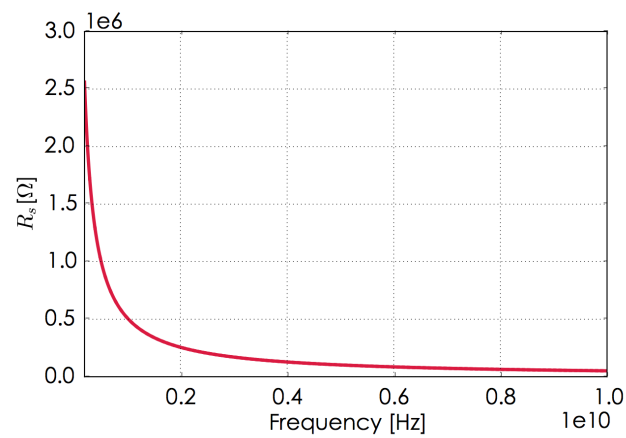

Figure 5: Maximum HOM shunt impedance producing a growth rate of the instability compensated by the natural radiation damping.

ELECTRON CLOUD STUDIES

Electron cloud (EC) has been recognized as one of the main limitations in the performance of the Large Hadron

ISBN 978-3-95450-187-8

Collider at CERN [9]. In the FCC-ee case, when the positron beam passes through a section of the accelerator, primary electrons can be produced by ionization of the residual gas in the beam pipe or by photoemission due to synchrotron radiations (photoelectrons). These primaries are attracted and accelerated by the beam up to energies of several hundreds of eV: when they impact the pipe walls with this energy, they produce secondary electrons that in turn, depending on their energy, can be absorbed, reflected, or accelerated again by the following bunch, thus producing an avalanche of electron multiplication. This accumulation of electrons in the beam chamber can represent another source of heat load and produce instabilities and emittance blow up. In this paper we will focus on the fast-head tail instability and on the heat load caused by the electron cloud in the two final focusing quadrupoles of the interaction region.

Heat Load due to Electron Cloud

In order to evaluate the EC build up in FCC-ee, we used the PyECLOUD code [10]. Table 3 shows the beam and magnet parameters used for electron cloud studies at 45.6GeV. In particular, by assuming an initial uniform distribution of electrons in the vacuum chamber, we simulated the following cases at 45.6 GeV:

- a train of 300 bunches with 2.5ns bunch spacing in both the symmetric and asymmetric layouts
- 30 trains of 8 bunches with 10ns gap and 2.5ns bunch spacing in the symmetric layout

Table 3: Beam and IR Magnet Parameters for FCC-ee at 45.6GeV

Energy [GeV]	**45.6**	
Bunch spacing [ns]	7.5	2.5
Bunch population [10^{11}]	1.0	0.33
H emittance [nm]	0.2	0.09
V emittance [pm]	1	1
Bunch length [mm]	6.7	3.8
Filling pattern	300b	(8b+4e)x30

	L[m]	G[T/m]	β_x[m]	β_y[m]
Quadrupole QC1R	3.2	26.6	53.3	8934
	1.6	46.2	34.6	10265
Quadrupole QC2R	2.5	18.7	341	4488
	2.5	16.3	297	4082

Fig. 6 shows the EC induced heat load for the two final magnets as a function of the Secondary Electron Yield for all the test cases. The multipacting threshold is $\simeq 1.1$ for both quadrupoles which means that we need a $SEY < 1.1$ to run the machine without electron cloud.
Simulations show that the heat load is up to three times lower for the quadrupole QC1R in the case of asymmetric layout while results in quadrupole QC2R confirmed that the presence of gaps in the bunch train allows to mitigate the electron cloud, with a heat load up to two times lower. One possibile strategy to avoid electron cloud in the machine will be the choice of a proper filling pattern that will depend also on HOMs considerations, as mentioned in the previous section.

Photoemission due to SR When charged particles are subject to a transverse acceleration, they emit photons that can have enough energy to extract electrons from the walls when hitting the pipe. Photoelectrons usually represent the main source of primaries in the EC build up. The number of photoelectrons that are generated per beam particle and per unit lenght is given by:

$$N_{ph} = N_\gamma Y \tag{6}$$

where

$$N_\gamma = \frac{5\alpha}{2\sqrt{3}}\frac{\gamma}{\rho} \tag{7}$$

is the number of photons per beam particle per unit length and Y is the Photoelectron Yield, i.e. the probability of electron emission per impinging photon. For FCC-ee, with a bending radius $\rho = 11.3$km, the number of photons per positron per meter is $N_\gamma = 0.085$ at 45.6GeV, a number three times higher than LHC at 7 TeV and roughly twice higher than FCC-hh at collision. Another fraction of photoelectrons is produced by the scattered photons and is associated to the photon reflectivity parameter R. The photoelectron yield and the photon reflectivity depend both on the pipe materials and synchrotron radiation properties. Since no experimental data exist for these parameters, simulations were performed by scanning Y and R in the following ranges: $Y = [0.05, 0.2, 0.3]$ and $R = [2\%, 50\%, 80\%]$. Results are shown in Fig. 7 for both quadrupoles by considering the 2.5ns beam at 45.6 GeV in the symmetric case.

Electron Density Threshold for the Single Bunch Head-tail Instability

The single bunch head-tail instability is the direct consequence of the interaction of the bunch with the electron cloud: if the bunch enters the e-cloud with the head slightly displaced from the beam axis, electrons will be attracted towards the head centroid position and there will be an accumulation of electrons in this region. Following particles of the bunch will be attracted by this new electron distribution and after few passages through the electron cloud the tail will be completely deflected [11].
Electron cloud acts as a short range wake field with frequency

$$\omega_e = \sqrt{\frac{2\lambda_p r_e c^2}{\sigma_y(\sigma_x + \sigma_y)}} \tag{8}$$

where $\lambda_p = \frac{N}{4\sigma_z}$ is the line density with N bunch population and σ_z bunch length, r_e is the classical electron radius

ISBN 978-3-95450-187-8

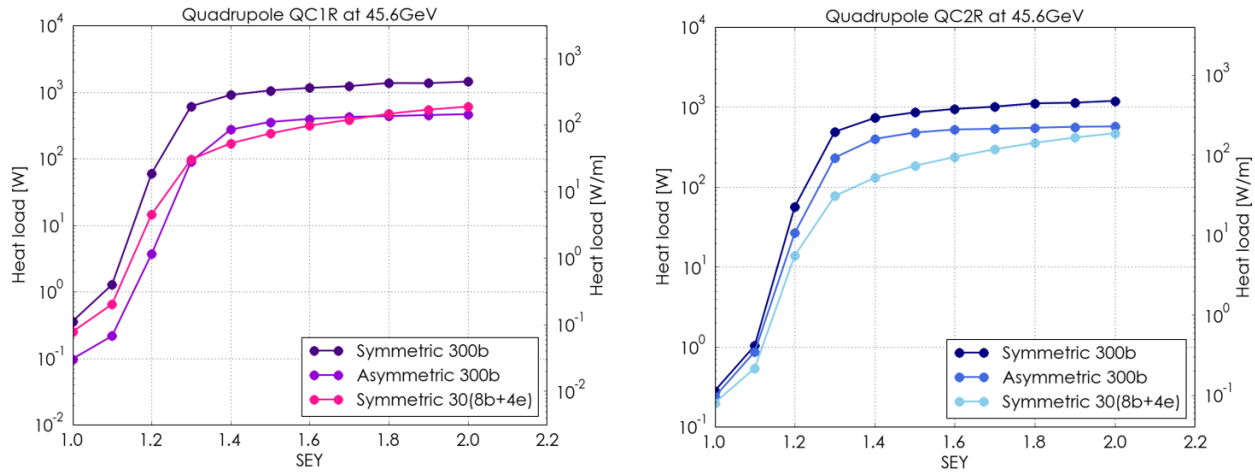

Figure 6: Heat load in the two final FCC-ee quadrupoles as a function of the SEY parameter at 45.6 GeV with 2.5ns bunch spacing.

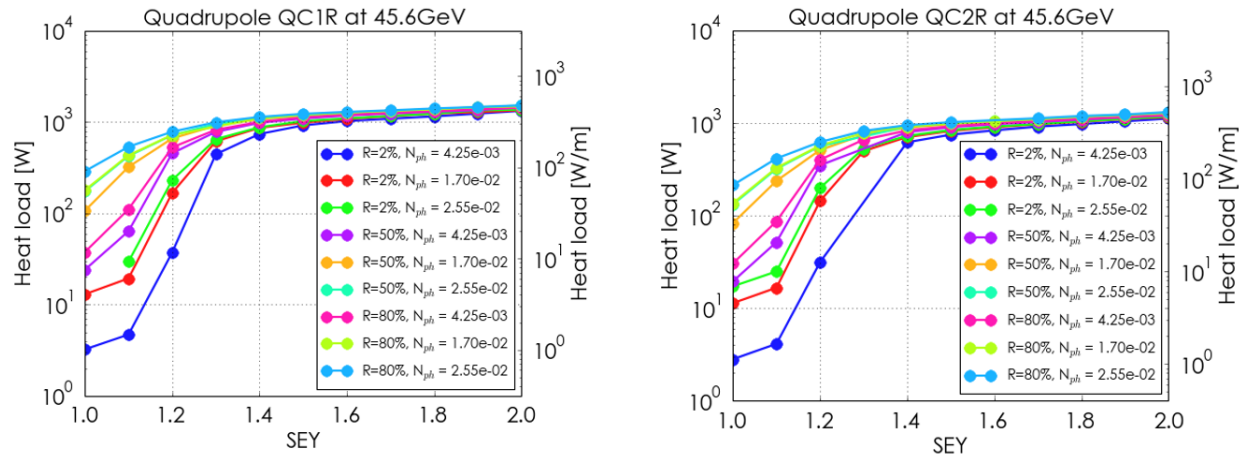

Figure 7: EC induced heat load as a function of the SEY for different values of the photon reflectivity and the photoelectron yield, for quadupole QC1R (on the left) and quadrupole QC2R (on the right) at 45.6 GeV with 2.5ns bunch spacing.

and $\sigma_{x,y}$ are the transverse beam dimensions.
The threshold density for the single bunch head - tail instability is given by

$$\rho_{th} = \frac{2\gamma\upsilon_s \frac{\omega_e \sigma_z}{c}}{\sqrt{3} K Q r_0 \beta C} \tag{9}$$

where υ_s is the synchrotron tune, C the machine circumference and we assumed $K = \frac{\omega_e \sigma_z}{c}$ and $Q = min(7, \frac{\omega_e \sigma_z}{c})$. Table 4 shows the parameters of FCC-ee for the lowest and highest energy cases and the corresponding density thresholds.

Table 4: FCC-ee Parameter List for Electron Density Threshold Evaluation

Energy [GeV]		**45.6**	**175**
Bunch spacing [ns]	7.5	2.5	4000
Bunch population [10^{11}]	1.0	0.33	1.7
Horizontal emittance [nm]	0.2	0.09	1.3
Vertical emittance [pm]	1	1	2.5
β [m]	100	100	100
Bunch length [mm]	6.7	3.8	2.5
Synchrotron tune	0.036	0.025	0.075
Elec. frequency $\frac{\omega_e}{2\pi}$ [GHz]	177.8	163	191.4
Elec. oscillation $\frac{\omega_e \sigma_z}{c}$	25	13	10
Density threshold [10^{10}]	**1.88**	**1.3**	**15**

CONCLUSIONS

Simulation results of the beam heat load contribution due to resistive wall and geometric impedances have been presented for the interaction region of FCC-ee. For the estimation of the power loss due to the resistive wall impedance we considered a pipe of aluminum and copper and in this latter case the losses are lower for all energies and below 60W/m (for the entire beam). ABCI simulations of the loss

ISBN 978-3-95450-187-8

factor of the synchotron radiation masks have also been performed, showing that the power loss is below 1W for all the energies. CST simulations in both time and frequency domains were performed to study high order modes in the IR, in particular the TM modes that remain trapped and can cause extra heating. In this context, the asymmetric layout seems to be the best choice, even if further studies are needed. Electron cloud induced heat load as a function of the SEY was estimated in the two final focusing quadrupoles of the interaction region by performing numerical simulation with the PyECLOUD code. Simulation results showed that the presence of gaps in the bunch train allows to mitigate the electron cloud in the machine. Moreover, the heat load is up to three times lower for both quadrupoles in the asymmetric layout case. The heat load was also estimated by scanning the photoelectron yield and the photon reflectivity. The multipacting threshold has been localized at 1.1 for both quadrupoles. An estimation of the electron density threshold of the single bunch head-tail instability was also presented. Further studies are needed to identify a possible strategy to mitigate the electron cloud: a scan of the bunch spacing and the use of different filling patterns will be analyzed more in detail.

ACKNOWLEDGEMENT

The authors would like to thank G. Iadarola, L.Mether, A.Romano, F. Zimmermann, K.Oide, K. Ohmi, M. Zobov, B. Salvant, N. Biancacci, E. Shaposhnikova, for their contribution and their valuable comments and discussions.

REFERENCES

[1] M.Sullivan, "FCC-ee Interaction Region Layout" FCC Week 2016, Rome, April 2016, http://indico.cern.ch/event/438866/contributions/1085089/

[2] K.Oide, "FCC-ee machine layout and optics" FCC Week 2016, Rome, April 2016, http://indico.cern.ch/event/438866/contributions/1085096/

[3] G. Rumolo, "Beam instabilities", Proceedings of the CAS-CERN Accelerator School: Advanced Accelerator Physics, Trondheim, Norway, 19–29 August 2013.

[4] N. Mounet, https://impedance.web.cern.ch/impedance/Codes/ImpedanceWake2D/user_manual_todate.txt

[5] Palumbo, L., Vittorio G. Vaccaro, and M. Zobov. "Wake fields and impedance." Arxiv preprint physics/0309023 (2003).

[6] http://abci.kek.jp/abci.htm

[7] A. Chao, et al., "Handbook of accelerator physics and engineering", World scientific, 2013.

[8] E.Belli, M.Migliorati, et al. "Single beam collective effects in FCC-ee due to beam coupling impedance." arXiv preprint arXiv:1609.03495 (2016).

[9] G. Iadarola, "Electron Cloud studies for CERN particle accelerators and simulation code development", PhD Thesis, Università degli Studi di Napoli Federico II, 2014

[10] https://github.com/PyCOMPLETE/PyECLOUD

[11] G. Rumolo and F. Zimmermann, "Theory and Simulation of the Electron cloud instability." Proceedings of the LHC Workshop Chamonix XI. 2001.

ISBN 978-3-95450-187-8